

Graphene-based three-body amplification of photon heat tunneling

Hamidreza Simchi*

*Department of Physics, Iran University of Science and Technology, Narmak, Tehran 16844, Iran and
Semiconductor Technology Center, P.O.Box 19575-199, Tehran, Iran*

(Dated: November 14, 2016)

We consider a three slabs configuration including two non-doped single layer graphene on insulating silicon dioxide (G/SiO₂) substrates and one non-doped suspended single layer graphene (SG). The suspended layer is placed between two G/SiO₂ layers. Without SG layer, the heat flux has maximum at Plasmon frequency supported by the G/SiO₂ slabs. In three slabs configuration, the photon heat tunneling is amplified between two G/SiO₂ layers significantly, only for specific range of vacuum gap between SG layer and G/SiO₂ layers and Plasmon frequency, due to the coupling of modes between each G/SiO₂ layer and SG layer. Since, the SG layer is a single atomic layer, the photon heat tunneling assisted by this configuration does not depend on the thickness of middle layer and in consequence, it can enable novel applications for nanoscale thermal management.

I. INTRODUCTION

In any material, there will be spontaneous electrical and magnetic moments that originate from quantum and thermal fluctuations. These fluctuating moments produce fluctuating electromagnetic fields inside and outside the material. One can calculate these fluctuating fields by adding a fluctuating induction terms to the Maxwell's equation [1]. Lifshitz has found the fields inside and outside the materials by using the fluctuation-dissipation theorem [2]. Since 1930, London has realized that quantum mechanical fluctuations of electric dipole moments could give rise to the force between bodies separated by macroscopic distances (van der Waals force) [3]. Abrikosova *et al.* have made the first direct measurements of the van der Waals force between macroscopic bodies [4]. The energy flow between two half spaces has been found using Lifshitz's method by using the Poynting vector rather than the Maxwell stress tensor [5]. Sipe has developed new Green function formalism for calculating fields generated by sources in the presence of a multi-layer geometry [6]. Narayanaswamy *et al.* have found a relation between cross-spectral densities of electromagnetic fields in thermal equilibrium and dyadic Green functions of the vector Helmholtz equation [7] and then generalized it to thermal non-equilibrium effects (i.e., when the objects are at different temperatures) and introduced a Green function formalism of energy and momentum transfer in fluctuational electrodynamics [8]. But, what will be the force and heat transfer between bodies separated by nanometer distances? Several groups [5, 9–11] have shown that when the gap distance, d between bodies becomes very small, the near-field heat transfer varies as d^{-2} . By using nonlocal dielectric function it has been shown that, the d^{-2} dependence would disappear for $d < 0.1$ nanometer (nm) [12], [13] but generally speaking, the nonlocal effects has little influence on the predicted heat flux for $d > 0.1$ nm [12]. Basu *et al.*

have considered two semi-infinite plates separated by a vacuum gap of finite width, especially for $0.1 < d < 100$ nm, and studied the dependency of maximum heat flux to the dielectric function and vacuum gap width [14]. In addition at subwavelength gap (i.e., in near field regime), it has been shown that, a significant increment of heat flux results from the evanescent photons which remain confined near the surface of the materials [15–22]. Messina *et al.*, have considered a metal-like (ML) medium layer (with width, δ) between two silicon carbide (SiC) layers (with width, d) and studied the amplification of photon heat tunneling in this structure [23]. They have shown that, only for $0.05 < \delta < 0.2$ micrometer (μm) and $0.05 < d < 0.3 \mu m$, the amplification was occurred [23]. The amplification of photon heat has opened new possibilities for development some technologies such as, thermophotovoltaic conversion devices [24, 25], Plasmon assisted nano-photolithography [26] and infrared sensing and spectroscopy [27, 28].

In the present work, we consider three-body configuration including a non-doped suspended single layer graphene (SG) which is placed between two non-doped single layer graphene on silicon dioxide (G/SiO₂) substrates. At first, we calculate the photon heat tunneling between two G/SiO₂ structure and show: how the heat flow depends on the value of gap (d) between these layers and frequency of field (ω). Then, we place the SG layer between these two G/SiO₂ structures, when the heat flux on SG layer is zero, and show that, the heat transfer between G/SiO₂ substrates is amplified only for specific range of vacuum gap between SG and each G/SiO₂ substrate i.e, d and Plasmon frequency. The structure of the article is as follows: in section II the analytical calculation method of dielectric constant of non-doped graphene and evanescent part of heat transfer will be presented. In section III the result and discussion and in section IV the summary will be provided, respectively.

* simchi@alumni.iust.ac.ir

II. ANALYTICAL CALCULATIONS

In this section of article, we provide the calculation method of dielectric constant and evanescent part of heat transfer.

A. Dielectric constant of undoped graphene

The expectation value of an arbitrary observable \hat{A} under the influence of a probe potential of the form:

$$\hat{V}(t) = \hat{B}F(t)\theta[t - t_0] \quad (1)$$

with \hat{B} being an observable, $F(t)$ a scalar function of time, and $\theta(t)$ the Heaviside step function, can be written as:

$$\delta\hat{A}(t) = \int_{-\infty}^{+\infty} \frac{d\omega}{2\pi} \chi_{AB}(\omega) F(\omega) e^{-i\omega t} \quad (2)$$

where $F(\omega)$ is Fourier transformation of $F(t)$ and $\chi_{AB}(\omega)$ is complex-valued generalized susceptibility, which is equal to:

$$\chi_{AB}(\omega) = -i \int_0^{+\infty} dt' [\hat{A}(t'), \hat{B}]_{eq} e^{i\omega t' - 0t'} \quad (3)$$

This quantity can be written with a slightly different, more convenient, notation as [29, 30]:

$$\chi(\vec{q}, \omega) = 4 \sum_{\alpha, \alpha'=\pm 1} \int \frac{d^2\vec{k}}{4\pi^2} \frac{(n_F(\alpha E_k) - n_F(\alpha' E_{k+q}))}{(\omega + \alpha E_k - \alpha' E_{k+q} + i\epsilon)} F_{\alpha\alpha'}(\vec{q}, \vec{k}) \quad (4)$$

where $\epsilon = 0^+$, $\alpha(\alpha')$ index of band, and

$$F_{\alpha\alpha'}(\vec{q}, \vec{k}) = \frac{1}{2} (1 + \alpha\alpha' \frac{k^2 + \vec{k} \cdot \vec{q}}{k |\vec{k} + \vec{q}|}) \quad (5)$$

$$n_F(E) = [e^{\beta\hbar\omega} + 1]^{-1} \quad (6)$$

where $\beta = (k_B T)^{-1}$, with T the temperature and k_B the Boltzmann constant. If θ is angle between \vec{k} and \vec{q} then

$$F_{\alpha\alpha'}(\vec{q}, \vec{k}) = \frac{1}{2} (1 + \alpha\alpha' \frac{k + q \cos(\theta)}{|\vec{k} + \vec{q}|}) \quad (7)$$

By changing the variable, $u = (1 + \alpha\alpha' \frac{k + q \cos(\theta)}{|\vec{k} + \vec{q}|})$ and using the below relations:

$$\omega - k = |\vec{k} + \vec{q}| \quad (8)$$

$$\cos(\theta) = \frac{(k + q \cos(\theta))}{(\omega - k)} \quad (9)$$

$$\sin(\theta) = \pm \frac{1}{2kq} \sqrt{4k^2q^2 - (\omega^2 - 2\omega k - q^2)^2} \quad (10)$$

The imaginary part of $\chi(\vec{q}, \omega)$ becomes (for $q < \omega$):

$$Im(\chi(\vec{q}, \omega)) = \frac{-1}{\pi \sqrt{\omega^2 - q^2}} \int_{\frac{\omega-q}{2}}^{\frac{\omega+q}{2}} dk \sqrt{q^2 - \omega^2 + 4k\omega - 4k^2} \quad (11)$$

But, $\sqrt{q^2 - \omega^2 + 4k\omega - 4k^2} = \sqrt{q^2 - (\omega + 2k)^2}$, and if $x \equiv |\vec{q}| / |\vec{k}_F|$ and $v = \omega/E_F$, it can be shown[30, 31]:

$$Im(\chi(\vec{q}, \omega)) = -\frac{x^2\theta(v-x)}{4\sqrt{v^2-x^2}}, q < \omega \quad (12)$$

$$Im(\chi(\vec{q}, \omega)) = 0, q > \omega \quad (13)$$

Also, based on the Kramers-Kronig relation, the relation between $Im(\chi(\vec{q}, \omega))$ and $Re(\chi(\vec{q}, \omega))$ is as follows[30]:

$$Re(\chi(\vec{q}, \omega)) = \frac{2}{\pi} P \int_0^\infty d\omega' \frac{\omega' Im(\chi(\vec{q}, \omega'))}{\omega'^2 - \omega^2} \quad (14)$$

where, P means principle vlaue. Therefore[30]:

$$Re(\chi(\vec{q}, \omega)) = -\frac{x^2\theta(x-v)}{4\sqrt{x^2-v^2}}, q > \omega \quad (15)$$

$$Re(\chi(\vec{q}, \omega)) = 0, q < \omega \quad (16)$$

However, based on the random phase approximation, the relation between dielectric constant $\varepsilon(\vec{q}, \omega)$ and susceptibility $\chi(\vec{q}, \omega)$ can be written as [31]:

$$\varepsilon(\vec{q}, \omega) = 1 - V(q)\chi(\vec{q}, \omega) \quad (17)$$

where, $V(q) = 2\pi e^2/\kappa q$ is the two dimensional Coulomb interaction. Therefore [31],

$$Re(\chi(\vec{q}, \omega)) = 1 + \frac{e^2}{2\varepsilon_0\varepsilon_r} (1 + x\theta(x \pm v)/(4\sqrt{x^2 - v^2})) \quad (18)$$

$$Im(\chi(\vec{q}, \omega)) = \frac{e^2}{2\varepsilon_0\varepsilon_r} x\theta(\pm v - x)/(4\sqrt{v^2 - x^2}) \quad (19)$$

Now, if $v > x$ then:

$$Re(\chi(\vec{q}, \omega)) = 1 + \frac{e^2}{2\varepsilon_0\varepsilon_r} \quad (20)$$

$$Im(\chi(\vec{q}, \omega)) = \frac{e^2}{2\varepsilon_0\varepsilon_r} x/(4\sqrt{v^2 - x^2}) \quad (21)$$

B. Evanescent photon heat tunneling

The three-body configuration is shown in Fig.1. First, we consider the structure without intermediate suspended graphene layer. We assume that the materials are nonmagnetic. It is obvious that, the electric and magnetic field that are generated by the component of the fluctuating induction $\vec{g}(\vec{r}, t)$ hold in the Maxwell's equations[5]

$$\nabla \times \vec{E}(\vec{r}, \omega) = i \frac{\omega}{c} \vec{H}(\vec{r}, \omega) \quad (22)$$

$$\nabla \times \vec{H}(\vec{r}, \omega) = -i \frac{\omega}{c} \vec{E}(\vec{r}, \omega) - i \frac{\omega}{c} \vec{g}(\vec{r}, t) \quad (23)$$

We can write the fields in terms of Fourier components as:

$$\vec{E} = \int_{-\infty}^{+\infty} \vec{a}(\vec{k}) e^{i\vec{k} \cdot \vec{r}} d\vec{k}, \vec{H} = \frac{c}{\omega} \int_{-\infty}^{+\infty} \vec{k} \times \vec{a}(\vec{k}) e^{i\vec{k} \cdot \vec{r}} d\vec{k} \quad (24)$$

and \vec{g} as:

$$\vec{g} = \int_{-\infty}^{+\infty} \vec{g}(\vec{k}) e^{i\vec{k} \cdot \vec{r}} d\vec{k} \quad (25)$$

By substituting Eqs.24 and 25 in Eqs.22 and 23, and defining the below vectors:

$$\vec{k}_{\pm} = \vec{q} \pm s_1 \hat{x}, \vec{q} = k_y \hat{y} + k_z \hat{z}, s_1 = \sqrt{\omega^2 \varepsilon_{SiO_2} - q^2} \quad (26)$$

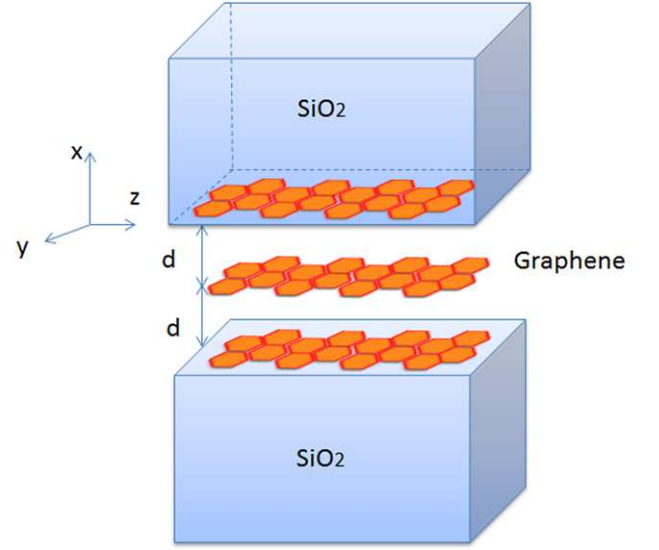


FIG. 1. Schematic of three-body configuration for photon heat tunneling calculation.

$$\hat{s} = \hat{q} \times \hat{x}, \hat{p}_{\pm} = k^{-1}(q\hat{x} \mp s_1\hat{q}) \quad (27)$$

$$\vec{\rho} = y\hat{y} + z\hat{z} \quad (28)$$

The transverse and parallel component of field become [5]:

$$\vec{E}^{\perp} = \int \frac{i\pi\omega^{SiO_2} t_{10}^{\perp}}{c^2 q^2 s_1} \exp[i\vec{q} \cdot \vec{\rho} + ipx] \times [\vec{g}(\vec{k}) \cdot (\vec{q} \times \hat{x})] (\vec{q} \times \hat{x}) d^2 q \quad (29)$$

$$\vec{E}^{\parallel} = \int \frac{i\pi\omega^{SiO_2} t_{10}^{\parallel}}{\sqrt{\varepsilon_{SiO_2}} q^2 s_1} \exp[i\vec{q} \cdot \vec{\rho} + ipx] \times [q^2 g_x(\vec{k}) - s_1 (\vec{q} \cdot \vec{g}(\vec{k}))] (q^2 \hat{x} - p\vec{q}) d^2 q \quad (30)$$

where, \vec{E}^{\perp} and \vec{E}^{\parallel} arise from the wave polarized perpendicular and parallel to the plane of incidence, respectively and t_{10}^{\perp} and t_{10}^{\parallel} are the transmission coefficients when the electric field is perpendicular and parallel to the plane of incidence, respectively. It can be shown that, if the vacuum width d satisfies in the below equation:

$$d \ll \frac{c}{2\omega \sqrt{|(1 - \varepsilon_{1,2})|}} \quad (31)$$

where, $\varepsilon_{1,2} = \varepsilon_{SiO_2}$ or ε_{SG} . The evanescent part of the heat flow, P_{ev} , is equal to[5]:

$$P_{ev} = \frac{\hbar}{\pi^2 d^2} \int_0^{\infty} \omega d\omega (n_B(E, T_1) - n_B(E, T_2)) \times \int_0^{\infty} \gamma d\gamma \frac{Im(\varepsilon_1) Im(\varepsilon_2)}{(|(\varepsilon_1 + 1)(\varepsilon_2 + 1) - (\varepsilon_1 - 1)(\varepsilon_2 - 1)e^{-\gamma}|)^2} e^{-\gamma} \quad (32)$$

Where, $\gamma = -2p\omega d/c$ and $n_B(E, T_i) = [e^{\hbar\omega} - 1]^{-1}$. If the SG layer is absent, then:

$$X \equiv \int_0^\infty \gamma d\gamma \frac{Im(\varepsilon_1)Im(\varepsilon_2)}{(|(\varepsilon_1 + 1)(\varepsilon_2 + 1) - (\varepsilon_1 - 1)(\varepsilon_2 - 1)e^{-\gamma}|)^2} e^{-\gamma} = \int_0^\infty \gamma d\gamma \frac{Im(\varepsilon_1)Im(\varepsilon_2)}{(|(\varepsilon_{G/SiO_2} + 1)^2 - (\varepsilon_{G/SiO_2} - 1)^2 e^{-\gamma}|)^2} e^{-\gamma} \quad (33)$$

X is radiative heat flux in the near-field and after normalization is shown by X^* [14]. In next section, we will use Eqs.20, 21, 32 and 33 for calculating P_{ev} .

III. NUMERICAL CALCULATIONS AND DISCUSSION

As an example, let us to consider two materials both with $-5 \leq Re(\varepsilon) \leq 5$ and $0.001 \leq Im(\varepsilon) \leq 10$ and study the heat flux between them. Fig.2(a) and (b) shows the normalized heat flux X^* when the thickness of gap d is equal to zero and 10 nm, respectively.

As Fig.2 shows, only for specific values of $Re(\varepsilon)$ and $Im(\varepsilon)$ heat flux is equal to one at $d = 0$ nm and decreases to the maximum value 0.01 at $d = 10$ nm due to the dependency of X^* to d . The result is in good agreement with the result of Ref.14. Now, we consider two G/SiO_2 layers and calculate the heat flux be-

tween them. Since, $k_B = 1.381 \times 10^{-23} m^2 K g s^{-2} K^{-1}$, $\hbar = 6.62 \times 10^{-34} m^2 K g s^{-1}$, $c = 3 \times 10^8 m s^{-1}$, and $T = 300 K$, therefore, $\omega = k_B T / \hbar = 3.932 \times 10^{13} s^{-1}$. Also, we know $\varepsilon_{SiO_2} = 4$ [23] then, by using Eqs. 20 and 21 we find:

$$Re(\varepsilon_{G/SiO_2}) = 1.125 \quad (34)$$

$$Im(\varepsilon_{G/SiO_2}) = \frac{e^2}{32} \frac{x}{\sqrt{v^2 - x^2}} \quad (35)$$

If we assume, for example $\varepsilon_{G/SiO_2} = 1.125 + i0.05$ then, the Eq.31 is satisfied for $d \ll 28.3 \times 10^{-6} m$. We assume $0 \leq d \leq 10 nm$ in next calculations.

Fig.3 shows contour plot of $\log_{10} X^*$ as a function of $Im(\varepsilon_{G/SiO_2})$ and d . Here, we assume $x = q/k_F = 1$, and $k_B = \hbar = e = 1$, for simplicity.

According to Fig.3, the heat flux reaches to 0.1 when imaginary part of dielectric constant is at range $0.20 < Im(\varepsilon) \leq 0.27$ and $0 \leq d \leq 7 nm$. In comparison with Fig.2, the heat flux increases by one order of magnitude. It means that the heat flux is amplified by choosing the G/SiO_2 structure. By using the value of $Im(\varepsilon)$ and Eq.28 we find $1.006 < v = \omega/E_F \leq 1.012$. On the Plasmon mode dispersion curve, the point $(q/k_F, \omega/E_F) = (1, 1.01)$ is placed on the boundaries of the single particle excitation (SPE) for intra- and inter-band electron excitation in graphene [31, 32]. Thus, the heat flux has a maximum at Plasmon frequency supported by the G/SiO_2 slabs.

Now let us to add the SG layer between two G/SiO_2 layers as Fig.1 shows. The total heat flow on SG layer

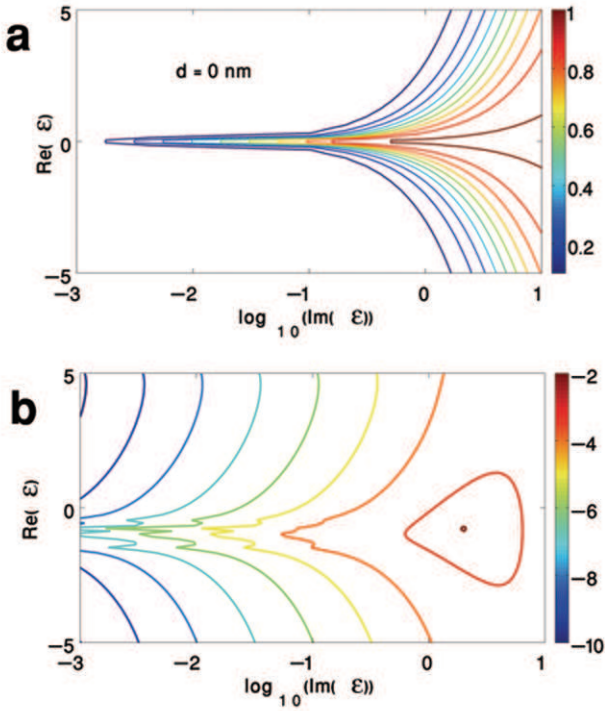


FIG. 2. (Color online) (a) Contour plot of X^* as a function of $Re(\varepsilon)$ and $Im(\varepsilon)$ at $d = 0 nm$ and (b) $\log_{10}(X^*)$ at $d = 10 nm$.

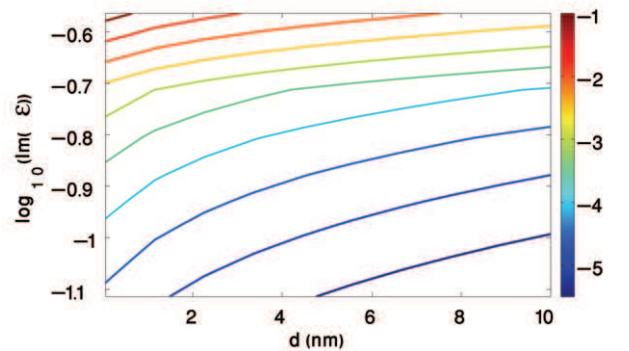


FIG. 3. (Color online) Contour plot of $\log_{10} X^*$ as a function of $Im(\varepsilon)$ and $d = 0 nm$.

from left G/SiO_2 layer is proportional to $[n_B(E, T_1) - n_B(E, T_2)]$ and the total heat flow on right G/SiO_2 layer from SG layer is equal to $[n_B(E, T_2) - n_B(E, T_3)]$. We choose the temperature T_2 the value such that the total heat flux on SG layer is zero i.e.,

$$n_B(E, T_1) - n_B(E, T_2) = n_B(E, T_2) - n_B(E, T_3) \quad (36)$$

or

$$T_2 = \frac{1}{k_B \hbar \omega} \text{Ln} \left[1 + \frac{2(e^{\beta_1 \hbar \omega} - 1)(e^{\beta_3 \hbar \omega} - 1)}{(e^{\beta_1 \hbar \omega} - 1) + (e^{\beta_3 \hbar \omega} - 1)} \right] \quad (37)$$

Here, we assume $T_1 = 300K$, $T_3 = 323K$. Fig.4 (a) shows the heat flux $\log_{10}[n_B(E, T_i) - n_B(E, T_j)]X^*$ between right (left) G/SiO_2 layer and SG layer and Fig.4 (b) shows the heat flux between two G/SiO_2 layers.

The heat flow between G/SiO_2 and SG layer is maximized for $d \rightarrow 0$ and $\omega/E_F \rightarrow 1$. Therefore, it is maximized at Plasmon frequency which is placed on the boundaries of the SPE for intra- and inter-band electron excitation (note, $x = q/k_F = 1$). As Fig.4 (b) shows,

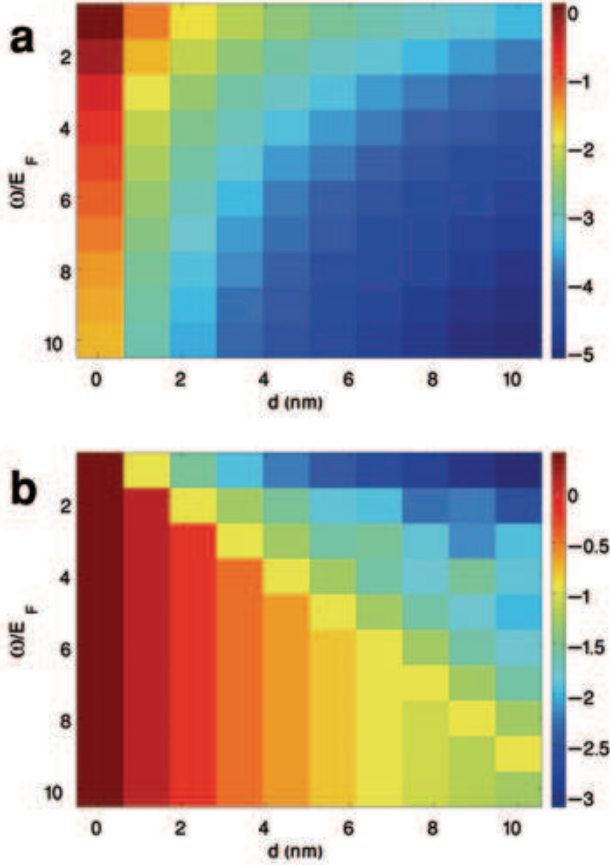


FIG. 4. (Color online) (a) Heat flux between G/SiO_2 layer and SG layer and (b) between two G/SiO_2 layers. Here, colorbar shows $\log_{10}[n_B(E, T_i) - n_B(E, T_j)]X^*$.

for $1 \leq \omega/E_F \leq 10$ and $d \leq 1nm$, then $[n_B(E, T_i) - n_B(E, T_j)]X^* \rightarrow 0.5$. Also for $2 \leq \omega/E_F \leq 10$ and $d \leq 3nm$, then $-0.5 < [n_B(E, T_i) - n_B(E, T_j)]X^* < 0.5$. It means that for a wide range of Plasmon frequency and gap thickness the heat flux has maximum. Finally, as Fig.5 shows, the ratio of heat flux after adding the SG layer to before adding the layer depends on ω/E_F and d but the heat flux is only amplified for specific range of ω/E_F and d by adding the intermediate SG layer.

It can be understood by looking at the coupling of modes between each G/SiO_2 layer and middle SG layer [23]. i.e., since the total heat transmission between two G/SiO_2 layers Φ_{13} is proportional to:

$$\Phi_{13} \propto [n_B(E, T_1) - n_B(E, T_2)]X^* + [n_B(E, T_2) - n_B(E, T_3)]X^* \quad (38)$$

and $n_{B,12} = n_{B,23} = n_{B,13}/2$, therefore $\tau_{13} = (\tau_{12} + \tau_{23})/2$ where τ_{ij} is the transmission probability between layer i and layer j [23].

IV. SUMMARY

We have considered a suspended graphene (SG) layer between two Graphene on SiO_2 layers (G/SiO_2) and studied the heat flux amplification between two G/SiO_2 layers. It has been shown that, before adding the SG layer, the heat flux had maximum at Plasmon frequency supported by the G/SiO_2 slabs. By adding the SG layer, the heat flux between two G/SiO_2 was amplified, for specific range of vacuum gap between SG layer and G/SiO_2 layers and Plasmon frequency, due to the modes coupling between each G/SiO_2 layer and middle SG layer. Since the intermediate SG layer was a single atomic layer, the heat transfer did not depend on the thickness of middle layer.

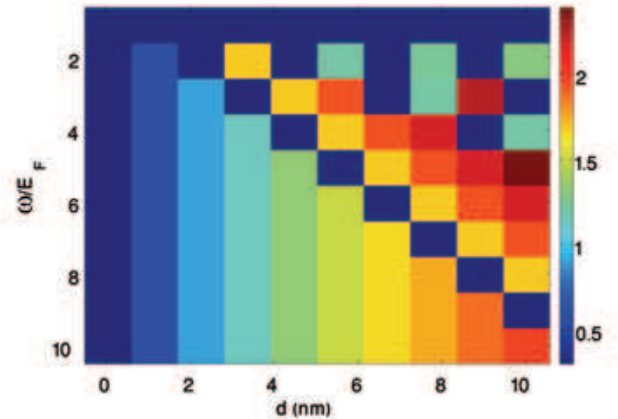


FIG. 5. (Color online) The ratio of heat flux after adding the SG layer to before adding the layer.

-
- [1] L. . Landau and E. M. Lifshitz, *Electrodynamics of Continuous Media* (Pergamon, New York, 1960).
 - [2] E. M. Lifshitz, Zh. Eksp. Teor. Fiz. **29**, 94 (1955).
 - [3] F. London, Z. Phys. **63**, 245 (1930).
 - [4] I. I. Abrikosova and B. V. Derjaguin, Dok. Akad. Nauk SSSR **90**, 1055 (1953).
 - [5] J. J. Loomis and H. J. Maris, Phys Rev. B **50**, 24 (1994).
 - [6] J. E. Sipe, J. Opt. Soc. Am. **4**, 4 (1987).
 - [7] A. Narayanaswamy and G. Chen, Quant. Spec. Radia. Tran. **111**, 1877 (2010).
 - [8] A. Narayanaswamy and Y. Zheng, Quant. Spec. Radia. Tran. **132**, 12 (2014).
 - [9] D. Polder and M. Vanhove, Phys Rev. B **4**, 3303 (1971).
 - [10] J. P. Mulet, K. Joulain, R. Carminati, and J. J. Greffet, Microscale Thermophys Eng. **6**, 209 (2002).
 - [11] C. J. Fu and Z. M. Zhang, Int. J. Heat Mass Transfer **49**, 1703 (2006).
 - [12] P. O. Chapuis, S. Volz, C. Henkel, K. Joulain, and J. J. Greffet, Phys. Rev. B **77**, 035431 (2008).
 - [13] A. I. Volokitin and B. N. J. Persson, Phys Rev. B **63**, 205404 (2001).
 - [14] S. Basu and Z. M. Zhang, J. Appl. Phys **105**, 093535 (2009).
 - [15] K. Joulain, J. P. Mulet, F. Marquier, R. Carminati, and J. J. Greffet, Surf. Sci. Rep. **57**, 59 (2005).
 - [16] A. I. Volokitin and B. N. J. Persson, Rev. Mod. Phys **79**, 1291 (2007).
 - [17] A. Kittle, W. Muller-Hirsch, J. Parisi, S. A. Biehs, D. Redding, and M. Holthaus, Phys Rev Lett. **95**, 224301 (2005).
 - [18] L. Hu, A. Narayanaswamy, X. Chen, and G. Chen, Appl. Phys. Lett. **92**, 133106 (2008).
 - [19] E. Rousseau, A. Siria, G. Jourdan, S. Volz, F. Comin, J. Chevrier, and J. J. Greffet, Nature Photon **3**, 514 (2009).
 - [20] S. Shen, A. Narayanaswamy, and G. Chen, Nano Lett. **9**, 2909 (2009).
 - [21] T. Kralik, P. Hanzelka, V. Musilova, A. Srnka, and M. Zobac, Rev. Sci. Instrum. **82**, 055106 (2011).
 - [22] R. S. Ottens, V. Quetschke, S. Wise, A. A. Alemi, R. Lundock, G. Mueller, D. H. Reitze, D. B. Tanner, and B. Whiting, Phys. Rev. Lett. **107**, 014301 (2011).
 - [23] R. Messina, M. Antezza, and P. Ben-Abdallah, (2012), qunt-ph/1205.2076v1.
 - [24] R. S. DiMatteo, P. Greiff, S. L. Finberg, K. A. Young-Waithe, H. K. H. Choy, M. M. Masaki, and C. G. Fonstad, Appl. Phys. Lett. **79**, 1894 (2001).
 - [25] A. Narayanaswamy and G. Chen, Appl. Phys. Lett. **82**, 3544 (2003).
 - [26] W. Srituravanich, N. Fang, C. Sun, Q. Luo, and X. Zhang, Nano Lett. **4**, 1085 (2004).
 - [27] Y. D. Wilde, F. Formanek, R. Carminati, B. Gralak, P. A. Lemoine, K. Goulain, J. P. Mulet, Y. Chen, and J. J. Greffet, Nature **444**, 740 (2006).
 - [28] A. C. Jones and M. B. Raschke, Nano Letters **12**, 1475 (2012).
 - [29] N. Nagaosa, *Quantum Field Theory in Condensed Matter Physics* (Springer, 1999).
 - [30] A. Scholz, *Charge and current response of spin-orbit coupled two-dimensional materials* (PhD Thesis, University of Regensburg, which can be downloaded on internet, 2013).
 - [31] E. H. Hwang and S. D. Sarma, (2007), cond-mat/0610561v3.
 - [32] M. Jablan, H. Buljan, and M. Soljacic, Phys Rev B **80**, 245435 (2009).